

A Model for Dipolar Glass and Relaxor Ferroelectric Behavior

Ronald Fisch¹

¹382 Willowbrook DR, North Brunswick, NJ 08902

(Dated: July 21, 2022)

Abstract

Heat bath Monte Carlo simulations have been used to study a 12-state discretized Heisenberg model with a type of random field, for several values of the randomness coupling parameter h_R . The 12 states correspond to the [110] directions of a cube. Simple cubic lattices of size $128 \times 128 \times 128$ with periodic boundary conditions were used, and 32 samples were studied for each value of h_R . The model has the standard nonrandom two-spin exchange term with coupling energy J and a field which adds an energy h_R to two of the 12 spin states, chosen randomly and independently at each site. We provide results for the cases $h_R/J = -2.5, -2.0, -1.5, 3.0$ and 4.0 . For all these cases except $h_R/J = -2.5$, we find a sharp phase transition at a temperature T_c where the specific heat and the longitudinal susceptibility are peaked. At T_c , the behavior of the peak in the structure factor, $S(\mathbf{k})$, at small $|\mathbf{k}|$ is a straight line on a log-log plot. However, the value of the slope of this line is not independent of h_r/J . Below T_c , the model has long-range ferroelectric order, and this order rapidly becomes oriented along one of the eight [111] directions as T is reduced. This rotation of the ordering direction is caused by the cubic anisotropy, which is a dangerous irrelevant variable. This creates a strong correction to ordinary critical scaling. For $h_R/J = -2.5$, we do not see clear evidence of a phase transition, but the spin correlation length becomes larger than $L = 128$ as T is reduced.

I. INTRODUCTION

The \mathbf{O}_{12} model[1, 2] is a model of discretized Heisenberg spins, *i.e.* \mathbf{O}_{12} is a discrete subgroup of $\mathbf{O}(\mathbf{3})$. We will put this model on a simple cubic lattice of size $L \times L \times L$, with periodic boundary conditions. It is now almost 25 years since the original Monte Carlo study[1] of the three-dimensional (3D) random field \mathbf{O}_{12} model. The numerical results presented there, which used $L \leq 64$, and studied four samples at two nonzero values of h_R , are crude by current standards. However, the reasons given for why this model is worthy of study are just as valid now as they were then. This model is designed to represent a ferroelectric dipolar glass,[3, 4] such as a random mixture of argon atoms and carbon monoxide molecules on a face-centered cubic lattice in which the concentration of carbon monoxide is greater than the percolation threshold. It is also believed to be relevant[5] for ferroelectric phases in strongly disordered perovskite alloys, which are often referred to as relaxor ferroelectrics.[6–11] From our point of view, the essential element for relaxor ferroelectric behavior is the alloy disorder, rather than a particular chemistry. A cubic perovskite which has a supercell ordering of a few perovskite unit cells in size should not be considered a relaxor ferroelectric, regardless of its chemical composition.

In the current paper, we extend our recent results[12] on a particular realization of this model. We have used the same computer program as before, although the procedures we follow have been slightly modified. We continue to study lattices of size $L = 128$, and we now present results for several values of the random field coupling parameter h_R . This gives a more complete picture of the phase diagram for this model.

Our Hamiltonian starts with the classical Heisenberg exchange form of a ferromagnet:

$$H_{ex} = -J \sum_{\langle ij \rangle} \mathbf{S}_i \cdot \mathbf{S}_j. \quad (1)$$

Each spin \mathbf{S}_i is a three-component dynamical variable which has twelve allowed states, which are unit vectors pointing the [110] directions of a cube. The $\langle ij \rangle$ indicates a sum over nearest neighbors on the simple cubic lattice. The symbol H , which denotes the uniform external field, does not appear explicitly in our Hamiltonian, because we have set H to zero. There is no loss of generality in setting $J = 1$. We will also set Boltzmann's constant to 1. This merely establishes the units of energy and temperature. The restriction of the spin variables to \mathbf{O}_{12} builds a temperature-dependent cubic anisotropy into the model. A useful review of

the effects of such a cubic anisotropy has been given by Pfeuty and Toulouse.[13]

We add to H_{ex} a random field which, at each site, is the sum of two Potts field terms:

$$H_{RP2} = h_R \sum_i (\delta_{\mathbf{s}_i, \hat{\mathbf{u}}_i} + \delta_{\mathbf{s}_i, \hat{\mathbf{v}}_i}). \quad (2)$$

Each $\hat{\mathbf{u}}_i$ and each $\hat{\mathbf{v}}_i$ is an independent quenched random variable. which assumes one of the twelve [110] allowed directions with equal probability. Since $\hat{\mathbf{u}}_i$ is allowed to be equal to $\hat{\mathbf{v}}_i$, the random field at each site has 78 possible types. The reader should note that, for an XY model, adding a second Potts field would generate nothing new, due to the Abelian nature of the $\mathbf{O}(2)$ group. However, in the current case, adding the second Potts field can substantially reduce the corrections to finite-size scaling.

Due to the way we have defined H_{RP2} , the energy per site of the system, E , does not go to zero as the temperature, T , goes to infinity. Actually, $E(T = \infty) = h_R/6$, and it would be straightforward to adjust the energy so that it would go to zero as $T \rightarrow \infty$ for any value of h_R . Although the reader might think it would be more natural to include a minus sign in H_{RP2} , the convention we are using is consistent with the definition used in our earlier work.[14]

The celebrated Imry-Ma construction,[15] argues that random fields built from groups with continuous symmetries cannot have conventional long-range order when the number of spatial dimensions is less than or equal to four. The Imry-Ma argument implicitly assumes that the spin group is Abelian. What is assumed is that the coupling of the random field to the spins is purely of vector form. However, at a renormalization group fixed point, a nonabelian random vector field has the ability to generate higher order tensor couplings to the effective spins. More specifically, the Imry-Ma argument does not consider the Halperin-Saslow anisotropy triad,[16] whose existence requires spins with at least three components. Whether or not such higher order couplings are relevant at the critical fixed point must be studied explicitly, on a case-by-case basis. One might expect that the Imry-Ma argument does not matter for our \mathbf{O}_{12} model. However, in the absence of the random field term, this model is in the universality class of the Heisenberg critical fixed point.[1, 13]

The results we find here demonstrate that the Imry-Ma instability does not necessarily exist for random fields applied to a Heisenberg model. For a nonabelian spin group the Halperin-Saslow effect[16] changes the long-wavelength dispersion from quadratic to linear. This can cure the Imry-Ma instability. This mechanism is also closely related to the ordering

in the 3D Heisenberg spin glass.[17] From the hydrodynamic viewpoint, a spin glass and a random field model for the same type of spins should have the same lower critical dimension. However, the Imry-Ma argument can only be applied to systems which do not have a Kramers degeneracy. The problem with the Imry-Ma argument for a random-field Heisenberg model is that for nonabelian spins the effect of two noncollinear random vector fields does not transform like a vector under rotations.

The reader may be tempted to object that the analysis of Halperin and Saslow should not be applicable in the presence of the cubic anisotropy. However, what we are really interested in here is the issue of the stability of the random-field Heisenberg critical point. It is believed that in 3D the pure Heisenberg critical point is stable against the presence of cubic anisotropy favoring the [111] directions.[13] For the \mathbf{O}_{12} model, this was verified numerically by the author.[1] Here we will demonstrate numerically that the necessary condition for the 3D random-field Heisenberg critical point to be stable against [111] cubic anisotropy is also satisfied. This form of cubic anisotropy is a type of "dangerous irrelevant variable", because it breaks the $O(3)$ symmetry of the Hamiltonian explicitly.

In the work presented here, we present results for $h_R = -2.5, -2.0, -1.5, 3.0$ and 4.0 . Note that having h_R positive means that \mathbf{S}_i has an increased energy if it points in the direction of $\hat{\mathbf{u}}_i$ or $\hat{\mathbf{v}}_i$. Thus for negative h_R there are usually 2 low energy states at each site, and for positive h_R there are usually 10 low energy states at each site. A natural consequence of this is that for h_R values of the same absolute value, the negative h_R has a stronger effect on the system than the positive h_R does, because confining a spin to 2 directions out of 12 is a much more serious restriction than confining a spin to 10 directions out of 12.

It is likely, however, that the qualitative nature of the thermodynamic phases will not depend on whether h_R is positive or negative, or even whether the values of h_R are equal for $\hat{\mathbf{u}}_i$ and $\hat{\mathbf{v}}_i$. Our results seem to support this expectation. In any case, the size of corrections to scaling are not universal. The author expects that corrections to scaling will be smallest when h_R is the same for both $\hat{\mathbf{u}}_i$ and $\hat{\mathbf{v}}_i$, because that is when the Halperin-Saslow effect is the strongest. Note that, with this type of a random field, the model does not become trivial in the limit $|h_R| \rightarrow \infty$.

The range of distributions of the random fields for which this effect will be found remains unclear. The pure Heisenberg critical point is not stable against the introduction of cubic anisotropy which favors the [100] directions. In that case, the phase transition becomes

first order.[13] However, a first-order phase transition with a latent heat is not allowed in a 3D model with quenched disorder.[18–20] The properties of such a "smeared first-order transition" are not yet well understood. The smearing out of the typical first order ferroelectric phase transition is essential for the high performance of relaxor ferroelectrics in applications.

II. NUMERICAL PROCEDURES

If h_R is chosen to be an integer, then the energy of any state of the model is an integer. Then it becomes straightforward to design a heat-bath Monte Carlo computer algorithm to study it which uses integer arithmetic for the energies, and a look-up table to calculate Boltzmann factors. This procedure substantially improves the performance of the computer program, and was used for all the calculations reported here. The program currently has the ability to use half-integer values of h_R . Lattices with periodic boundary conditions were used throughout.

Three different linear congruential random number generators are used. The first chooses the $\hat{\mathbf{u}}_i$, the second chooses the $\hat{\mathbf{v}}_i$ and the third is used in the Monte Carlo routine which flips the spins. The generator used for the spin flips, which needs very long strings of random numbers, was the Intel library program *random_number*. In principle, Intel *random_number* can be used for multicore parallel processing. However, our program is so efficient in single-core mode that no speedup was seen when the program was run in parallel mode. The code was checked by correctly reproducing the known results[1] of the $h_R = 0$ case, and extending them to $L = 128$.

For each value of h_R , 32 samples of size $L = 128$ were studied. The same set of 32 samples was used for all values of T , so it is meaningful to talk about heating and cooling of each sample. Each sample was initially placed in a random state, and then cooled slowly. Both cooling and heating were done in temperature steps of 0.015625, with times of 20,480 Monte Carlo steps per spin (MCS) at each stage. (The reader should note that the temperatures we use in the computer code are simple binary fractions, even though they may appear to be unnatural when written in decimal notation.)

For the pure \mathbf{O}_{12} system, the Heisenberg critical temperature[1] is $T_c = 1.453$. For $h_R = 3$, the spin correlations are only short-ranged above this temperature, so no extended data runs

were made in this region of T . For 30 of the 32 samples studied, the system was strongly oriented along one of the [111] directions by the time it had been cooled to $T = 1.3125$. The other two samples had become trapped in metastable states. These two samples were then initialized in [110] states which had a positive overlap of approximately 0.5 with their metastable states. They were run at $T = 1.25$, where they were easily able to relax to low energy [111] states. These states were then warmed slowly to $T = 1.4375$. At $T = 1.34375$, these [111] states were seen to have significantly lower energies than the metastable states found by cooling for those two samples.

The fact that it was not difficult to find a stable state oriented along [111] at $T = 1.25$ means that, for $h_R = 3$, an $L = 128$ sample does not have many metastable states. However, it is expected that for large enough values of L it should be true that in the [111] ferroelectric phase there would be a metastable state corresponding to each of the [111] directions. It is to be expected that this might no longer be true when $|h_R|$ becomes large. In the proposed power-law correlated phase,[1] it would no longer be possible to assign low-energy metastable states to particular [111] directions.

Trial runs made on $L = 64$ lattices allowed us to estimate the range of T of most interest for each value of h_R which was studied. In the $h_R = 0$ case, we know that there is a first order phase transition from a [111] ordered phase to a [110] ordered phase. However, a detailed study of the behavior of this second transition was not undertaken. At low temperatures, the presence of h_R makes it difficult to tell when the system has equilibrated. In any case, the existence of the lower transition depends on the details of the model, so it is probably not relevant to experimental systems.

A data collection run for each sample consisted of a relaxation stage and a data stage. Except for T values high enough so that correlations were much smaller than the sample size, a relaxation stage was a run of length 122,880 MCS. In many cases this was sufficient to bring the sample to an apparent local minimum in the phase space. This was followed by a data collection stage of the same length. If further relaxation was observed during the data collection stage, it was reclassified as a relaxation stage. Then a new data collection stage was run. The energy and magnetization of each sample were recorded every 20 MCS. A spin state of the sample was saved after each 20,480 MCS. Thus there were six spin states saved from the data collection stage for each run. These six spin states were Fourier transformed and averaged to estimate the structure factor for each sample. At the high values of T , a

relaxation stage of only 20,480 MCS was judged to be sufficient.

III. THERMODYNAMIC FUNCTIONS

For a random field model, unlike a random bond model, the average value of the local spin, $\langle \mathbf{S}_i \rangle$, is not zero even in the high-temperature phase. The angle brackets here denote a thermal average. Thus the longitudinal part of the susceptibility, $\chi_{||}$, is given by

$$T\chi_{||}(\mathbf{k}) = 1 - |\mathbf{M}|^2 + L^{-3} \sum_{i \neq j} \cos(\mathbf{k} \cdot \mathbf{r}_{ij}) (\mathbf{S}_i \cdot \mathbf{S}_j - Q_{ij}), \quad (3)$$

For Heisenberg spins,

$$Q_{ij} = \langle \mathbf{S}_i \rangle \cdot \langle \mathbf{S}_j \rangle, \quad (4)$$

and

$$|\mathbf{M}|^2 = L^{-3} \sum_i Q_{ii} = L^{-3} \sum_i [\langle \mathbf{S}_i \rangle \cdot \langle \mathbf{S}_i \rangle]_t. \quad (5)$$

where the square brackets $[\dots]_t$ indicate a time average. Q_{ij} must be included for all T . Note that the $\chi_{||}$ we define here is not exactly what would be called the longitudinal susceptibility in a nonrandom system. The distinction between longitudinal modes and transverse modes is not completely well-defined in a system which has a local order parameter that is not fully aligned with the sample-averaged order parameter. In any case, the cubic anisotropy suppresses the soft modes in our system below T_c , in the ferroelectric phase.

These equations are not adequate in the limit $L \rightarrow \infty$ when there is a phase transition, if the low temperature phase contains multiple Gibbs states. If multiple Gibbs states exist at some T , then each $\langle \mathbf{S}_i \rangle$ must acquire an index κ , which specifies the Gibbs state to which it belongs. Each Q_{ij} will inherit this same index, *i.e.* $Q_{ij} \rightarrow Q_{ij}^\kappa$. For our model, κ specifies one of the eight [111] directions. Our data reported here are taken at fixed $L = 128$, and we did not attempt to find systematically the local minima corresponding to all the [111] directions. This would not even be possible for $L = 128$ at T only a small amount below the apparent T_c . Under those conditions a sample can often find its most stable local minimum within the time we run our Monte Carlo algorithm. Thus we do not need to include κ explicitly in the analysis of our data.

The specific heat, c_H , may be calculated by taking the finite differences $\Delta E / \Delta T$, where E is the energy per spin. Alternatively, it may be calculated as the variance of E divided by T^2 . The second method was used for the c_H numbers shown in our tabulated data.

A. Weak Random Field Strength

If the value of $|h_R|$ is very small, then it is necessary to use samples of very large L , in order for the system to get through the crossover from pure system behavior and show the true random field behavior. It was found empirically that $h_R = -1.5$ and $h_R = 3.0$ were satisfactory choices for $L = 128$ samples. The thermodynamic data calculated from our Monte Carlo data on the 32 $L = 128$ samples for $h_R = 3$ are shown in Table I. There are some small differences between these data and the original tabulation shown for $h_R = 3$ in the earlier paper,[12] because a stricter criterion for deciding that a sample had reached equilibrium was used here. This table now includes the results for both the hot start and cold start runs at $T = 1.40625$. In addition, for the case $T = 1.390625$, the prior report accidentally averaged over only 22 of the 32 samples which have been calculated.

The data in Table I show that there are peaks in $\chi_{||}$ and c_H at T_c . However, accurate estimates of the values of the correlation length critical exponent, ν , would require collecting a lot more data at temperatures close to T_c . As we shall see, our data below T_c do not have the form of typical critical scaling behavior. This may be partly a reflection of the fact that this type of model is expected to show replica-symmetry breaking[21] (RSB) below T_c . It has been understood for a long time that, in a mean-field approximation, RSB is a type of ergodicity breaking.[22, 23] We are very far from mean-field theory here, however.

Define $M_x(t)$, $M_y(t)$ and $M_z(t)$ to be the averages over the lattice at time t of the components of \mathbf{S}_i , in the usual way. Then the cubic orientational order parameter (COO) is measured by calculating the quantity

$$COO = 3[(M_x^2 M_y^2 + M_x^2 M_z^2 + M_y^2 M_z^2)/|\mathbf{M}|^4]_t. \quad (6)$$

where the brackets $[...]_t$ indicate an average over time as well as an average over samples. The possible values of COO range from 0 when \mathbf{M} points in a $[100]$ direction to 1 when \mathbf{M} points along a $[111]$ direction. Note that if all of the spins were fully aligned along one of the $[110]$ directions, the value of COO would be $3/4$. Table I shows that the sample average of COO is approximately 0.60 in the paraelectric phase, and that it rapidly increases to 1 as T is reduced below T_c . This behavior indicates that the $[111]$ orientational ordering is irrelevant at the random-field Heisenberg critical point, just as it is irrelevant at the pure Heisenberg critical point.

Table I: Thermodynamic data for $128 \times 128 \times 128$ lattices at $h_R = 3.0$, for various T . (h) and (c) signify data obtained relaxing from hotter and colder initial conditions, respectively. The one σ statistical errors shown are due to the sample-to-sample variations.

T	$ \mathbf{M} $	$\chi_{ }$	E	c_H	COO
1.34375(c)	0.427 ± 0.002	25.5 ± 3.6	-1.1955 ± 0.0001	2.784 ± 0.009	0.985 ± 0.006
1.375 (c)	0.311 ± 0.004	86.0 ± 7.8	-1.1047 ± 0.0002	2.997 ± 0.012	0.869 ± 0.029
1.390625(c)	0.230 ± 0.004	151 ± 19	-1.0569 ± 0.0001	3.111 ± 0.016	0.722 ± 0.041
1.40625(c)	0.125 ± 0.005	304 ± 37	-1.0072 ± 0.0002	3.182 ± 0.018	0.620 ± 0.040
1.40625(h)	0.124 ± 0.006	346 ± 43	-1.0072 ± 0.0002	3.184 ± 0.023	0.611 ± 0.040
1.4375 (h)	0.0238 ± 0.0012	72.4 ± 1.7	-0.9173 ± 0.0001	2.472 ± 0.009	0.599 ± 0.012

The structure factor, $S(\mathbf{k}) = \langle |\mathbf{M}(\mathbf{k})|^2 \rangle$, for Heisenberg spins is

$$S(\mathbf{k}) = L^{-3} \sum_{i,j} \cos(\mathbf{k} \cdot \mathbf{r}_{ij}) \mathbf{S}_i \cdot \mathbf{S}_j, \quad (7)$$

where \mathbf{r}_{ij} is the vector on the lattice which starts at site i and ends at site j . When there is a phase transition into a state with long-range spin order, $S(\mathbf{k} = 0)$ has a stronger divergence than $\chi(\mathbf{k} = 0)$ does.

Values of $S(|\mathbf{k}|)$ calculated by taking an angular average for each sample and then averaging the results for the 32 $L = 128$ samples. In Fig. 1, the results for $S(|\mathbf{k}|)$ at the 15 smallest non-zero values of $|\mathbf{k}|$ are shown as a function of T using a log-log plot. For larger $|\mathbf{k}|$ the slope of S becomes less negative, because the system is then in the crossover region between the pure system fixed point and the random-field fixed point. Note that the data shown for the cold initial condition and the hot initial condition at $T = 1.40625$ are virtually indistinguishable. At lower temperatures, two of the hot initial condition samples became trapped in metastable states for times accessible to our calculations. For this reason, we do not show the hot initial condition data for $T < 1.40625$.

For the range of $|\mathbf{k}|$ shown in Fig. 1, the fact that the straight-line fit to the data for $T = 1.40625$ is essentially perfect is remarkable. This is only a numerical accident, however, since we did not tune the temperature to find this condition. The fit of the hot initial condition data to a straight line has a slope of -2.788 ± 0.014 , and the fit to the cold initial condition data has a slope of -2.786 ± 0.016 . Averaging these gives

$$-(4 - \bar{\eta}) = -2.787 \pm 0.014 \quad (8)$$

as the slope of $S(|\mathbf{k}|)$ on the log-log plot at the critical point in the scaling region. We do not reduce our error estimate, because the data for the different initial conditions on the same set of samples cannot be considered to be statistically independent. Thus, at $h_R = 3$

$$\bar{\eta} = 1.213 \pm 0.014, \quad (9)$$

which is a reasonable value for this quantity. The value of $\bar{\eta}$ should not be sensitive to varying T by a small amount away from $T = 1.40625$. This is shown by the fact that the data in Fig. 1 for $T = 1.390625$ run parallel to the data for $T = 1.40625$ over a range of $|\mathbf{k}|$, and for smaller $|\mathbf{k}|$ the slope of $S(|\mathbf{k}|)$ becomes more negative. What this means is that $\bar{\eta}$ is not a continuous function of T . We are not seeing a critical phase of the Kosterlitz-Thouless type, for which $\bar{\eta}$ would be decreasing continuously as T decreases below T_c .

The thermodynamic data for $h_R = -1.5$, shown in Table II, are generally very similar to the data for $h_R = 3$. The value of T_c now appears to be slightly higher than $T = 1.40625$. We see again that there are peaks in $\chi_{||}$ and c_H at T_c , and that the COO parameter increases rapidly toward 1 as T decreases below T_c .

Table II: Thermodynamic data for $128 \times 128 \times 128$ lattices at $h_R = -1.5$, for various T . (h) and (c) signify data obtained relaxing from hotter and colder initial conditions, respectively. The one σ statistical errors shown are due to the sample-to-sample variations.

T	$ \mathbf{M} $	$\chi_{ }$	E	c_H	COO
1.359375(c)	0.407 ± 0.002	24.6 ± 2.1	-1.4483 ± 0.0001	2.848 ± 0.011	0.985 ± 0.006
1.375 (c)	0.352 ± 0.003	47.7 ± 4.0	-1.4027 ± 0.0001	2.983 ± 0.010	0.947 ± 0.011
1.390625(c)	0.277 ± 0.004	92.2 ± 7.7	-1.3550 ± 0.0002	3.096 ± 0.012	0.858 ± 0.027
1.40625(c)	0.177 ± 0.006	273 ± 48	-1.3051 ± 0.0002	3.233 ± 0.019	0.721 ± 0.034
1.421875(c)	0.073 ± 0.004	240 ± 9	-1.2554 ± 0.0001	3.043 ± 0.016	0.619 ± 0.028
1.4375 (h)	0.0291 ± 0.0015	95.1 ± 3.3	-1.2117 ± 0.0001	2.548 ± 0.011	0.598 ± 0.019

In Fig. 2, the results for $S(|\mathbf{k}|)$ at the 15 smallest non-zero values of $|\mathbf{k}|$ for $h_R = -1.5$ are shown as a function of T again using a log-log plot. The picture is similar to Fig. 1, except that the curvature in $S(|\mathbf{k}|)$ for T just below T_c is less visible. This, combined with the slightly higher value of T_c , suggest that $L = 128$ may not be quite large enough to complete the full crossover to random field critical behavior when $h_R = -1.5$.

The fit of the hot initial condition data for $T = 1.40625$ to a straight line has a slope of -2.735 ± 0.024 , and the fit to the cold initial condition data has a slope of -2.767 ± 0.021 . Averaging these gives

$$-(4 - \bar{\eta}) = -2.751 \pm 0.021 \quad (10)$$

as the slope of $S(|\mathbf{k}|)$ on the log-log plot at the critical point in the scaling region. Thus,

$$\bar{\eta} = 1.249 \pm 0.021 \quad (11)$$

at $h_R = -1.5$. Although the agreement for the values of $\bar{\eta}$ for these two values of h_R , -1.5 and 3.0, is pretty good, that is not convincing evidence of $\bar{\eta}$ being independent of h_R , because these two values of h_R were both chosen to be about as small as we could expect to be able to get meaningful results for at $L = 128$. For a proper test of the universality of $\bar{\eta}$, we need results for other values of h_R .

B. Intermediate Random Field Strength

Now we show results for $h_R = 4.0$ and $h_R = -2.0$, so that $|h_R|$ is somewhat larger. The thermodynamic data for $h_R = 4.0$, shown in Table III, are qualitatively similar to the data for $h_R = 3.0$. The value of T_c now appears to be somewhat lower than $T = 1.390625$. We see again that there are peaks in $\chi_{||}$ and c_H at T_c , and that the COO parameter increases toward 1 as T decreases below T_c .

Table III: Thermodynamic data for $128 \times 128 \times 128$ lattices at $h_R = 4.0$, for various T . (h) and (c) signify data obtained relaxing from hotter and colder initial conditions, respectively. The one σ statistical errors shown are due to the sample-to-sample variations.

T	$ \mathbf{M} $	$\chi_{ }$	E	c_H	COO
1.34375(c)	0.345 ± 0.005	59 ± 5	-1.1821 ± 0.0002	2.798 ± 0.008	0.874 ± 0.024
1.359375(c)	0.276 ± 0.006	101 ± 10	-1.1372 ± 0.0002	2.880 ± 0.014	0.763 ± 0.040
1.375 (c)	0.203 ± 0.006	146 ± 10	-1.0912 ± 0.0002	2.963 ± 0.014	0.678 ± 0.044
1.375 (h)	0.199 ± 0.007	163 ± 15	-1.0911 ± 0.0002	2.958 ± 0.013	0.660 ± 0.045
1.390625(c)	0.115 ± 0.006	183 ± 17	-1.0437 ± 0.0002	3.016 ± 0.014	0.612 ± 0.040
1.390625(h)	0.115 ± 0.006	271 ± 27	-1.0437 ± 0.0002	3.030 ± 0.014	0.599 ± 0.039
1.40625(h)	0.057 ± 0.004	160 ± 6	-0.9969 ± 0.0001	2.939 ± 0.015	0.570 ± 0.028
1.421875(h)	0.030 ± 0.002	84 ± 2	-0.9534 ± 0.0001	2.628 ± 0.011	0.598 ± 0.017

In Fig. 3, the results for $S(|\mathbf{k}|)$ at the 15 smallest non-zero values of $|\mathbf{k}|$ for $h_R = 4.0$ are shown as a function of T , again using a log-log plot. Our best estimate of T_c for $h_R = 4.0$ is slightly below $T = 1.390625$. The slope of $S(|\mathbf{k}|)$ on the log-log plot for $T = 0.390625$ is -2.848 ± 0.20 for the hot initial condition, and -2.850 ± 0.20 for the cold initial condition. Averaging these results gives

$$-(4 - \bar{\eta}) = -2.849 \pm 0.020 \quad (12)$$

for the slope of the log-log plot and

$$\bar{\eta} = 1.151 \pm 0.020 \quad (13)$$

at $h_R = 4.0$. This value is not consistent with the values of $\bar{\eta}$ which we found for the weak h_R cases.

At $T = 1.375$ the Fig. 3 data for $S(|\mathbf{k}|)$ are close to a straight line with a slope which is close to -3.0 . In Fig. 4, we show data for $|\mathbf{k}|^3 S(|\mathbf{k}|)$ over a range of $|\mathbf{k}|$ on a linear plot, for a range of T around T_c . It shows that below T_c there a range of T for which $|\mathbf{k}|^3 S(|\mathbf{k}|)$ is approximately constant over the range of $|\mathbf{k}|$ shown. This range cannot extend all the way to $|\mathbf{k}| \rightarrow 0$ because there is a sum rule for $S(|\mathbf{k}|)$. In any case, we expect that the crystalline cubic anisotropy must suppress $S(|\mathbf{k}|)$ for small enough $|\mathbf{k}|$.

Now we discuss the data for the case $h_R = -2.0$. The thermodynamic data are displayed in Table IV. For this case, we extend the range of data down to $T = 1.25$, which is low enough so that the system's behavior is reaching the strong COO limit. Our best estimate of T_c for $h_R = -2.0$ is slightly below $T = 1.375$, where the agreement between the data using

the hot initial condition and the cold initial condition is again fairly good. We also show similar data for $T = 1.359375$, where the agreement is not so good. This is again caused by 2 of the 32 hot initial condition samples becoming stuck in metastable states when the temperature is lowered below T_c .

Table IV: Thermodynamic data for $128 \times 128 \times 128$ lattices at $h_R = -2.0$, for various T . (h) and (c) signify data obtained relaxing from hotter and colder initial conditions, respectively. The one σ statistical errors shown are due to the sample-to-sample variations.

T	$ \mathbf{M} $	$\chi_{ }$	E	c_H	COO
1.25 (c)	0.535 ± 0.002	11.0 ± 1.4	-1.7927 ± 0.0001	2.282 ± 0.007	0.996 ± 0.001
1.28125(c)	0.472 ± 0.003	23.2 ± 2.0	-1.7189 ± 0.0001	2.420 ± 0.009	0.974 ± 0.006
1.3125 (c)	0.390 ± 0.004	52.4 ± 6.1	-1.6401 ± 0.0002	2.608 ± 0.012	0.920 ± 0.013
1.328125(c)	0.332 ± 0.006	62.4 ± 5.1	-1.5987 ± 0.0002	2.676 ± 0.011	0.816 ± 0.037
1.34375(c)	0.269 ± 0.007	99 ± 10	-1.5559 ± 0.0002	2.750 ± 0.012	0.706 ± 0.047
1.359375(c)	0.193 ± 0.008	174 ± 20	-1.5119 ± 0.0002	2.842 ± 0.013	0.691 ± 0.039
1.359375(h)	0.187 ± 0.009	162 ± 17	-1.5118 ± 0.0002	2.838 ± 0.012	0.648 ± 0.045
1.375 (c)	0.120 ± 0.007	207 ± 16	-1.4668 ± 0.0001	2.901 ± 0.013	0.642 ± 0.036
1.375 (h)	0.120 ± 0.007	215 ± 17	-1.4668 ± 0.0001	2.900 ± 0.013	0.636 ± 0.035
1.390625(h)	0.067 ± 0.004	159 ± 8	-1.4217 ± 0.0001	2.840 ± 0.011	0.611 ± 0.032
1.40625(h)	0.037 ± 0.002	92 ± 2	-1.3785 ± 0.0001	2.661 ± 0.011	0.593 ± 0.028

In Fig. 5, the results for $S(|\mathbf{k}|)$ at the 15 smallest non-zero values of $|\mathbf{k}|$ for $h_R = -2.0$ are shown as a function of T , again using a log-log plot. Our best estimate of T_c for $h_R = -2.0$ is slightly below $T = 1.375$. The slope of $S(|\mathbf{k}|)$ on the log-log plot for $T = 0.390625$ is -2.869 ± 0.30 for the hot initial condition, and -2.862 ± 0.33 for the cold initial condition. Averaging these results gives

$$-(4 - \bar{\eta}) = -2.866 \pm 0.030 \quad (14)$$

for the slope of the log-log plot and

$$\bar{\eta} = 1.134 \pm 0.030 \quad (15)$$

at $h_R = -2.0$. Therefore, it appears to be well established that the value of $\bar{\eta}$ is not independent of h_R for this model. However, the trend for negative h_R is the same as for

positive h_R , although the rate of change of $\bar{\eta}$ with h_R is larger when h_R is negative. This confirms our *a priori* expectations.

We do not have a simple explanation of the variation of $\bar{\eta}$ along the T_c versus h_R line. However, the author cannot resist the observation that this effect reminds him of the Angell plot,[24] which shows that the freezing behavior of "strong glasses" differs from the behavior of "fragile glasses". (Note that the Angell plot uses the symbol η for viscosity, which is not related to our notation.)

In Fig. 6, we show the $h_R = -2.0$ data for $|\mathbf{k}|^3 S(|\mathbf{k}|)$ over a range of $|\mathbf{k}|$ on a linear plot. It shows that below T_c there a range of T for which $|\mathbf{k}|^3 S(|\mathbf{k}|)$ is approximately constant over a range of $|\mathbf{k}|$, as in Fig. 4. For lower T the slope is positive, because the long-range order is being stabilized by the COO. We expect that Fig. 4 would also show this stabilization if we had data for lower values of T in the $h_R = 4.0$ case. We also expect that the weak random field cases would show similar behavior for values of L sufficiently larger than 128.

C. Strong Random Field Strength

For large positive h_R , H_{RP2} acts like a constraint which forbids 2 of the 12 states, chosen randomly at each site, from being occupied. Since 2 is much smaller than 12, this constraint is probably not strong enough to destroy long-range order at low temperatures. The situation for large negative h_R is very different. In that case, only 2 of the 12 states on each site are allowed. Such a model does not have the Kramers degeneracy, and it is not expected to be in a spin-glass universality class. However, this does not mean it would be trivial to find the ground state(s) of the model. It is known that a necessary condition for the existence of a finite temperature phase transition into a state which possesses true long-range order is that there be more than one thermodynamic Gibbs state in the low temperature phase. In the absence of Kramers degeneracy, it is not clear that this condition can be satisfied. On the other hand, there is no proper proof that a glass-type phase transition cannot exist in our model at finite T in 3D. This issue is very similar to the question of whether the de Almeida-Thouless line exists in a 3D Ising spin-glass,[25] or the Gabay-Toulouse line exists in a Heisenberg spin-glass.[26]

Thermodynamic data for $h_R = -2.5$ are displayed in Table V. We do not show data for $T < 1.25$, because we do not have confidence in the ability of our calculations to provide

meaningful results within accessible relaxation times at lower T . What these data show is that there is no single value of T which can be identified as T_c . The peak in $\chi_{||}$ is not occurring at the same T as the peak in c_H . The COO does not start increasing until a even lower T , of about 1.3. We would need a larger value of L to be able to know if the COO goes to 1 for $h_R = -2.5$. The author is not able to do such a calculation at this time.

Table V: Thermodynamic data for $128 \times 128 \times 128$ lattices at $h_R = -2.5$, for various T . (h) and (c) signify data obtained relaxing from hotter and colder initial conditions, respectively. The one σ statistical errors shown are due to the sample-to-sample variations.

T	$ \mathbf{M} $	$\chi_{ }$	E	c_H	COO
1.25 (c)	0.311 ± 0.007	56 ± 5	-1.8686 ± 0.0002	2.295 ± 0.008	0.721 ± 0.033
1.28125(c)	0.204 ± 0.011	84 ± 6	-1.7941 ± 0.0002	2.419 ± 0.009	0.672 ± 0.039
1.296875(c)	0.159 ± 0.010	110 ± 8	-1.7555 ± 0.0002	2.483 ± 0.010	0.648 ± 0.040
1.3125 (c)	0.121 ± 0.007	125 ± 7	-1.7160 ± 0.0001	2.535 ± 0.008	0.580 ± 0.044
1.328125(c)	0.085 ± 0.006	134 ± 8	-1.6757 ± 0.0001	2.608 ± 0.011	0.588 ± 0.039
1.34375(h)	0.059 ± 0.004	109 ± 5	-1.6350 ± 0.0001	2.620 ± 0.009	0.580 ± 0.035
1.359375(h)	0.041 ± 0.003	76 ± 2	-1.5945 ± 0.0001	2.562 ± 0.011	0.583 ± 0.034

We did not find any value of T for which the $h_R = -2.5$ data looked like a good straight line on a log-log plot, which is consistent with the lack of a well-defined T_c in Table V. It is clear that the entire sample is strongly correlated at $T = 1.25$, but this does not prove true long-range order for $L \rightarrow \infty$. In Fig. 7 and Fig. 8, we show how $|\mathbf{k}|^3 S(|\mathbf{k}|)$ versus $|\mathbf{k}|$ changes with T . The hot initial condition data of Fig. 7 show that $|\mathbf{k}|^3 S(|\mathbf{k}|)$ increases as T decreases, but the slope of the data at small $|\mathbf{k}|$ remains positive. The data for the cold initial condition, which extend down to $T = 1.25$, show a more complicated picture. The small $|\mathbf{k}|$ data for $T = 1.25$ are no longer rising as T decreases. This most likely indicates merely that we would need a larger value of L to see the true small $|\mathbf{k}|$ behavior at this T .

IV. DISCUSSION

The procedures we follow may be thought of as a hybrid of $\vec{\mathbf{k}}$ renormalization group ideas and finite-size scaling. The connection is made through the use of the fast Fourier transform,

which requires that L be a power of two. Looking at the small- $|\mathbf{k}|$ part of $S(|\mathbf{k}|)$ allows us to select out the part of the Monte Carlo data which contains information about the long-wavelength behavior, and ignore the crossover from pure system behavior to random-field behavior, which dominates the shorter wavelengths. That is necessary, because there is no good reason to expect that this crossover can be modelled by a simple correction-to-scaling functional form. This does not mean we are assuming anything about whether we will find some kind of a critical point. As we have seen, no critical behavior was found in our calculation for the case $h_R = -2.5$.

In order to understand the significance of our results, it is necessary to explain carefully how the RP2 \mathbf{O}_{12} model is related to the random-field Ising model (RFIM). It was shown by Aharony[27] that a small uniform uniaxial will cause an isotropic or cubic model in a random field to cross over to the RFIM universality class. Extensive numerical calculations by Fytas and Martin-Mayor[28, 29] have shown that the 3D RFIM has a well-behaved critical point which obeys universality. It must be pointed out, however, that what Fytas and Martin-Mayor did was show that the fourth cumulant of the randomness probability distribution was an irrelevant variable at the RFIM critical point, and the calculate the critical exponents for that case. Generalizing the ideas of Lubensky,[30] we expect that all cumulants of the fixed point random-field probability distribution need to be considered.

For example, the author does not believe it is obvious that a Cauchy distribution should give the same critical exponents for the RFIM as the ones found by Fytas and Martin-Mayor. Even more interesting is the situation for a random-field distribution which is not symmetric, so that it breaks the Z_2 symmetry. In that case, it should be expected that the 5D RFIM model has a weakly first-order phase transition. A first-order transition for the RFIM in 3D is not allowed,[18–20] but one should not expect universality to hold for the 3D RFIM if the random-field distribution breaks the Z_2 symmetry. The author does not know of any existing material which is an example of this, but does not think it is forbidden by any physical principle. It seems only slightly more unusual than a chiral crystal, and less exotic than a quasicrystal.

Thus it should not be considered a big surprise that our results for $\bar{\eta}$ for the RP2 \mathbf{O}_{12} model do not obey universality. The author does not think it to be any more surprising than the results for a 3D random-field 3-state Potts model not showing universality. In this context, it should be noted that Hui and Berker[20] claimed that the phase transition in a

3D random model should be a critical point, since such a model cannot have a first-order transition. However, it is not clear that Hui and Berker intended to imply that such a phase transition should have universal critical exponents. Turkoglu and Berker[31] have revisited this model, but they do not calculate critical exponents. A recent calculation of critical exponents for the model has been given by Kumar, Banerjee, Puri and Weigel,[32] who use the zero-temperature method. The latter calculation studies only one type of random field, so there is no test for universality of these critical exponents.

V. CONCLUSION

In this work we have used Monte Carlo computer simulations to study a model of discretized Heisenberg spins on simple cubic lattices in 3D, with a carefully chosen type of random field. We have found that, if the strength of the random field is not too large, our system shows a sharp critical point and a transition into a phase with long-range order. The phase transition shows characteristics expected of random field behavior. However, the value of the critical exponent $\bar{\eta}$, which describes the scaling of $S(|\mathbf{k}|)$ at T_c is not independent of h_R .

This example shows that the extreme difficulty in reaching equilibrium which is usually associated with glassy behavior is not an inevitable consequence of the presence of random fields. Standard renormalization group arguments imply that a similar transition ought to exist in a 3D model of this type with continuous spins and random fields which have an isotropic probability distribution. The primary reason why the existence of such behavior has been considered impossible until now is that the nonabelian nature of the $\mathbf{O}(\mathbf{3})$ group, which can give rise to relevant higher order tensor couplings to the random field, was not properly taken into account. We have also identified the relaxor ferroelectric effect as arising from a strong correction to scaling of the ferroelectric order parameter near T_c , which is probably caused by the cubic anisotropy, a dangerous irrelevant variable, which is present in this model and also in real cubic perovskite relaxor ferroelectrics. This strong correction to scaling may not occur in a model with isotropic spins and an isotropic distribution of random fields, or in an experimental system which is not a crystalline alloy.

Acknowledgments

This work used the Extreme Science and Engineering Discovery Environment (XSEDE) through allocation DMR180003. Bridges Regular Memory at the Pittsburgh Supercomputer Center was used for some preliminary code development, and the new Bridges-2 Regular Memory machine was used to obtain the data discussed here. The author thanks the staff of the PSC for their help.

-
- [1] R. Fisch, Phys. Rev. **B 57**, 269 (1998).
 - [2] R. Fisch, Phys. Rev. **B 58**, 5684 (1998).
 - [3] U. T. Hochli, K. Knorr and A. Loidl, Adv. Phys. **39**, 405 (1990).
 - [4] K. Binder and J. D. Reger, Adv. Phys. **41**, 547 (1992).
 - [5] B. I. Halperin and C. M. Varma, Phys. Rev. **B 14**, 4030 (1976).
 - [6] G. A. Smolenskii and V. A. Isupov, Dokl. Acad. Nauk SSSR **97**, 653 (1954) [Sov. Phys. Doklady **9**, 653 (1954)].
 - [7] G. Burns and F. H. Dacol, Phys. Rev. **B 28**, 2527 (1983).
 - [8] V. Westphal, W. Kleemann, and M. D. Glinchuk, Phys. Rev. Lett. **68**, 847 (1992).
 - [9] W. Kleemann, Int. J. Mod. Phys. **B 7**, 2469 (1993).
 - [10] R. Pirc, B. Tadic and R. Blinc, Phys. Rev. **B 36**, 8607 (1987).
 - [11] R. Pirc and R. Blinc, Phys. Rev. **B 60**, 13470 (1999).
 - [12] R. Fisch, Phys. Rev. **E 105**, 014102 (2022).
 - [13] P. Pfeuty and G. Toulouse, *Introduction to the Renormalization Group and to Critical Phenomena*, (John Wiley & Sons, Chichester, UK, 1977), Chapter 9, pp. 131-139.
 - [14] R. Fisch, Phys. Rev. **B 67**, 094110 (2003).
 - [15] Y. Imry and S.-K. Ma, Phys. Rev. Lett. **35**, 1399 (1975).
 - [16] B. I. Halperin and W. M. Saslow, Phys. Rev. **B 16**, 2154 (1977).
 - [17] L. A. Fernandez, V. Martin-Mayor, S. Perez-Gaviro, A. Tarancon and A. P. Young, Phys. Rev. **B 80**, 024422 (2009).
 - [18] M. Aizenman and J. Wehr, Phys. Rev. Lett. **62**, 2503 (1989); *ibid.* **64**, 1311(E) (1990).
 - [19] M. Aizenman and J. Wehr, Commun. Math. Phys. **130**, 489 (1990).

- [20] K. Hui and A. N. Berker, Phys. Rev. Lett. **62**, 2507 (1989).
- [21] M. Mezard and A. P. Young, Europhys. Lett. **18**, 653 (1992).
- [22] H. Sompolinsky and A. Zippelius, Phys. Rev. **B 25**, 6860 (1982).
- [23] H.-J. Sommers, Z. Phys. **B 50**, 97 (1983).
- [24] C. A. Angell, Science **267**, **5602**, 1924 (1995).
- [25] J. R. O. de Almeida and D. J. Thouless, J. Phys. **A 11**, 983 (1978).
- [26] M. Gabay and G. Toulouse, Phys. Rev. Lett. **47**, 201 (1981).
- [27] A. Aharony, Phys. Rev. **B 18**, 3328 (1978).
- [28] N. G. Fytas and V. Martin-Mayor, Phys. Rev. Lett. **110**, 227201 (2013).
- [29] N. G. Fytas and V. Martin-Mayor, Phys. Rev. **E 93**, 063308(2016).
- [30] T. C. Lubensky, Phys. Rev. **B 11**, 3573 (1975).
- [31] A. Turkoglu and A. N. Berker, J. Phys. **A 583**, 126339 (2021).
- [32] M. Kumar, V. Banerjee, S. Puri and M. Weigel, arXiv:2205.13047v2.

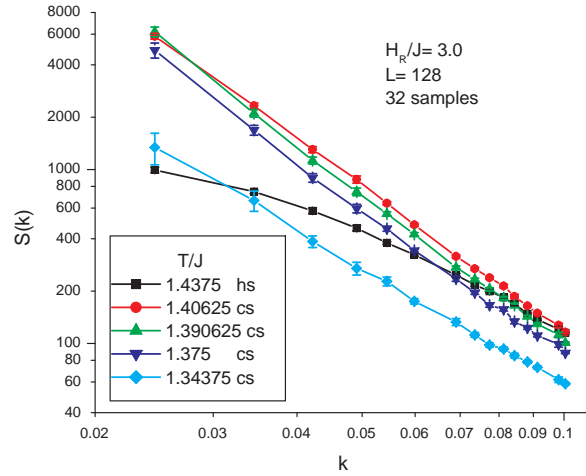


FIG. 1: Angle-averaged structure factor, $S(|\mathbf{k}|)$, at a sequence of temperatures for the RP2 \mathbf{O}_{12} model with $h_R = 3.0$ on $128 \times 128 \times 128$ simple cubic lattices, log-log plot. The points show averaged data from 32 samples, at a series of temperatures. (hs) and (cs) signify data obtained by relaxing from hotter and colder initial conditions, respectively.

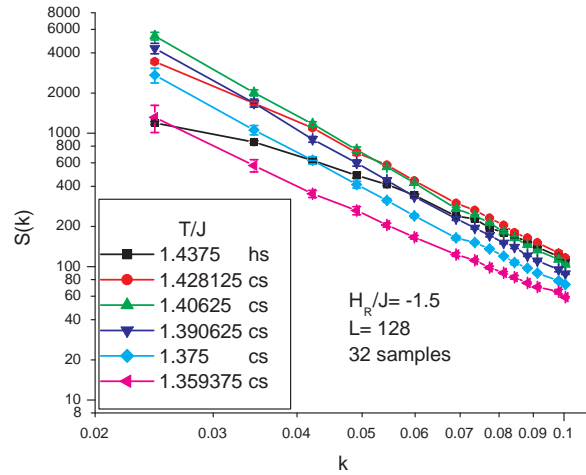


FIG. 2: Angle-averaged structure factor, $S(|\mathbf{k}|)$, at a sequence of temperatures for the RP2 \mathbf{O}_{12} model with $h_R = -1.5$ on $128 \times 128 \times 128$ simple cubic lattices, log-log plot. The points show averaged data from 32 samples. (hs) and (cs) signify data obtained by relaxing from hotter and colder initial conditions, respectively.

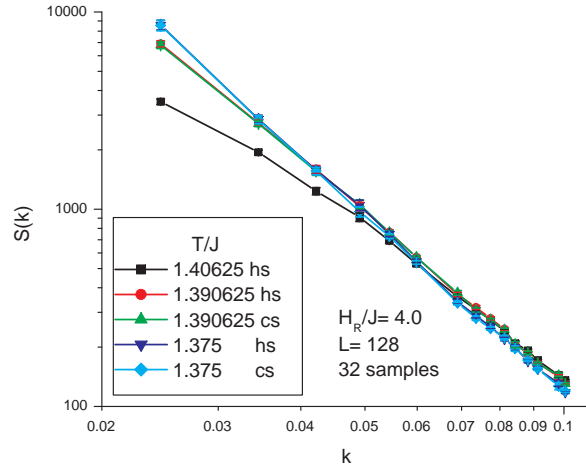


FIG. 3: Angle-averaged structure factor, $S(|\mathbf{k}|)$, at a sequence of temperatures for the RP2 \mathbf{O}_{12} model with $h_R = 4.0$ on $128 \times 128 \times 128$ simple cubic lattices, log-log plot. The points show averaged data from 32 samples, at a series of temperatures. (hs) and (cs) signify data obtained by relaxing from hotter and colder initial conditions, respectively.

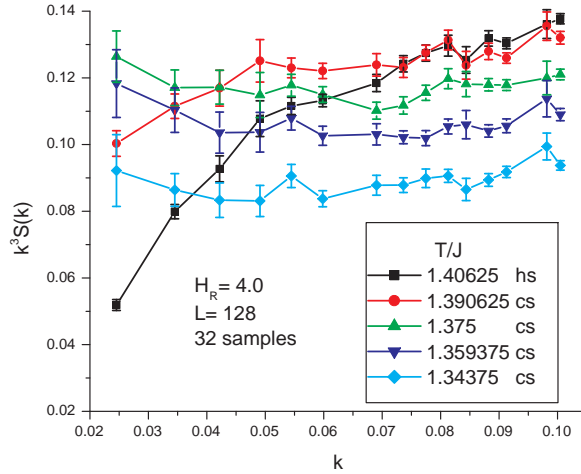


FIG. 4: Angle-averaged structure factor, $S(|\mathbf{k}|)$, at a sequence of temperatures for the RP2 \mathbf{O}_{12} model with $h_R = 4.0$ on $128 \times 128 \times 128$ simple cubic lattices. The points show averaged data from 32 samples. (hs) and (cs) signify data obtained by relaxing from hotter and colder initial conditions, respectively.

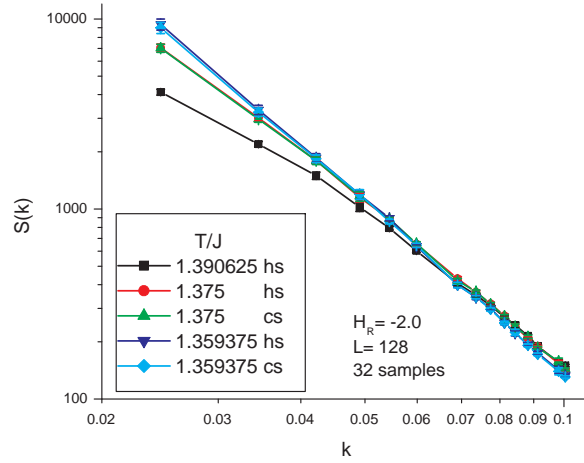


FIG. 5: Angle-averaged structure factor, $S(|\mathbf{k}|)$, at a sequence of temperatures for the RP2 \mathbf{O}_{12} model with $h_R = -2.0$ on $128 \times 128 \times 128$ simple cubic lattices, log-log plot. The points show averaged data from 32 samples, at a series of temperatures. (hs) and (cs) signify data obtained by relaxing from hotter and colder initial conditions, respectively.

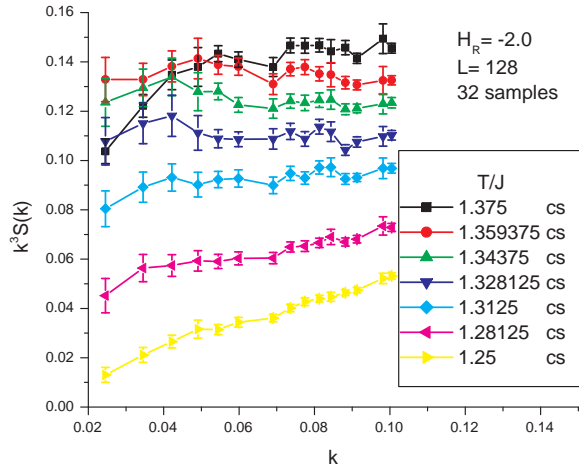


FIG. 6: Angle-averaged structure factor, $S(|\mathbf{k}|)$, at a sequence of temperatures for the RP2 \mathbf{O}_{12} model with $h_R = -2.0$ on $128 \times 128 \times 128$ simple cubic lattices. The points show averaged data from 32 samples. (hs) and (cs) signify data obtained by relaxing from hotter and colder initial conditions, respectively.

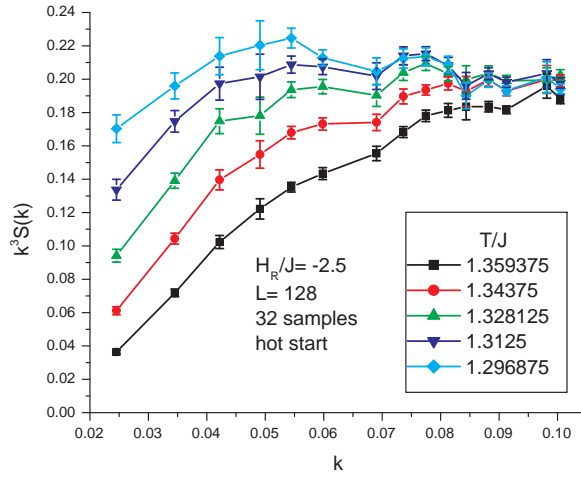


FIG. 7: Angle-averaged structure factor, $S(|\mathbf{k}|)$, at a sequence of temperatures for the RP2 \mathbf{O}_{12} model with $h_R = -2.5$ on $128 \times 128 \times 128$ simple cubic lattices. The points show averaged data from 32 samples. These data were obtained by relaxing from hotter initial conditions.

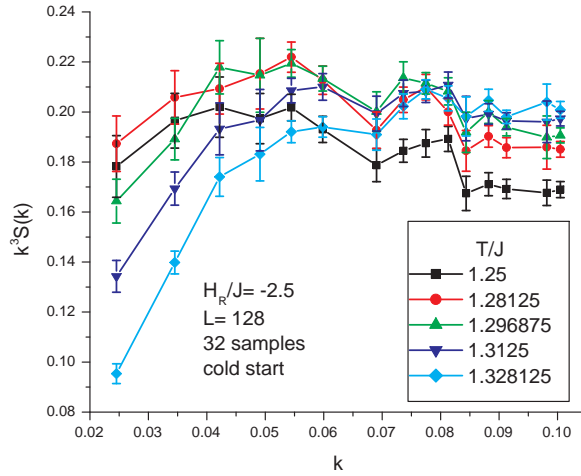


FIG. 8: Angle-averaged structure factor, $S(|\mathbf{k}|)$, at a sequence of temperatures for the RP2 \mathbf{O}_{12} model with $h_R = -2.5$ on $128 \times 128 \times 128$ simple cubic lattices. The points show averaged data from 32 samples. These data were obtained by relaxing from colder initial conditions.